The origin of ferroelectricity in magnetoelectric $YMnO_3$

BAS B. VAN AKEN*[1], THOMAS T. M. PALSTRA[1], ALESSIO FILIPPETTI†[2] AND NICOLA A. SPALDIN‡[2]

[1]Materials Science Centre, University of Groningen, Nijenborgh 4, 9747 AG, Groningen, The Netherlands
[2]Materials Department, University of California, Santa Barbara, California 93106-5050, USA
*Present address: Department of Materials Science and Metallurgy, University of Cambridge, New Museums Site, Pembroke Street, Cambridge CB2 3QZ, UK
†Present address: Dipartimento di Fisica, Università di Cagliari and INFM-Laboratorio Regionale di Fisica Computazionale, I-09042 Monserrato, Italy
‡e-mail: nicola@mrl.ucsb.edu

Published online: 22 February 2004; doi:10.1038/nmat1080

Understanding the ferroelectrocity in magnetic ferroelectric oxides is of both fundamental and technological importance. Here, we identify the nature of the ferroelectric phase transition in the hexagonal manganite, $YMnO_3$, using a combination of single-crystal X-ray diffraction, thorough structure analysis and first-principles density-functional calculations. The ferroelectric phase is characterized by a buckling of the layered MnO_5 polyhedra, accompanied by displacements of the Y ions, which lead to a net electric polarization. Our calculations show that the mechanism is driven entirely by electrostatic and size effects, rather than the usual changes in chemical bonding associated with ferroelectric phase transitions in perovskite oxides. As a result, the usual indicators of structural instability, such as anomalies in Born effective charges on the active ions, do not hold. In contrast to the chemically stabilized ferroelectrics, this mechanism for ferroelectricity permits the coexistence of magnetism and ferroelectricity, and so suggests an avenue for designing novel magnetic ferroelectrics.

Ferroelectric materials have a spontaneous electric polarization that can be switched by an applied electric field. They are used in a wide range of applications, including data storage and as capacitors, transducers and actuators, as a result of their wide variety of physical and electronic properties[1,2]. Most technologically important ferroelectrics are perovskite structure oxides, but there is increasing interest in the class of ferroelectric hexagonal manganites as non-volatile memory materials[3], as gate ferroelectrics in field-effect transistors[4] and because of their coupled magnetic and ferroelectric behaviour[5]. In addition to their technological relevance, the fundamental physics of ferroelectrics is rich and fascinating. In particular, many ferroelectrics undergo a phase transition from a high-temperature, high-symmetry phase that behaves as an ordinary dielectric, to the spontaneously polarized phase at low temperature, and a great deal of research has focused on understanding the nature of, and driving force for, these ferroelectric phase transitions.

In fact, perovskite structure oxides in which the bonding is entirely ionic are always centrosymmetric (and therefore not ferroelectric). This is because the short-range Coulomb repulsions between electron clouds on adjacent ions are minimized for centrosymmetric structures. The existence or absence of a ferroelectric instability is therefore determined by a balance between these short-range repulsions, which favour the non-ferroelectric centrosymmetric structure, and additional bonding considerations, which act to stabilize the ferroelectric phase.

Currently two distinctly different chemical mechanisms for stabilizing the distorted structures in ferroelectric oxides have been identified. Both are described as second-order Jahn-Teller effects in the literature, see for example ref. 6. The first is the ligand-field hybridization of a transition metal cation by its surrounding anions. This is the origin of the off-centre displacement of the small cation in the common perovskite ferroelectrics such as $BaTiO_3$ and $Pb(Zr,Ti)O_3$. It was first identified theoretically[7,8] in $PbTiO_3$ and $BaTiO_3$, and was described as a Ti 3*d*–O 2*p* hybridization. Note that this mechanism requires that the *d* orbitals on the small cation are formally unoccupied, and so precludes the coexistence of ferroelectricity and magnetism[9]. The second mechanism occurs around cations that have an $(ns)^2$ valence electron configuration. The tendency of $(ns)^2$ ions to lose inversion symmetry is well established, with the conventional explanation invoking a mixing

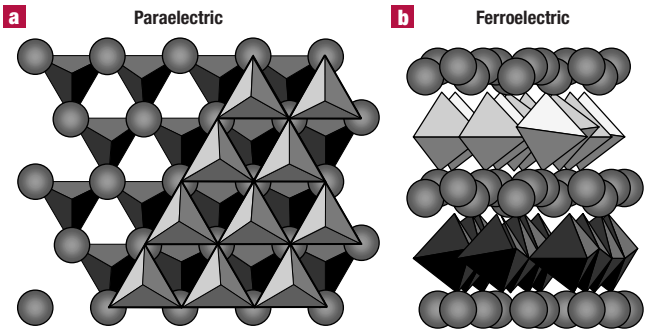

Figure 1 The crystal structure of $YMnO_3$ in the paraelectric and ferroelectric phases. The trigonal bipyramids depict MnO_5 polyhedra and the spheres represent Y ions. **a**, The stacking of two consecutive MnO_5 layers and the sandwiched Y layer, looking down the *c* axis in the paraelectric phase. **b**, A view of the ferroelectric phase from perpendicular to the *c* axis, showing the layered nature of $YMnO_3$.

between the $(ns)^2$ ground state and a low-lying $(ns)^1(np)^1$ excited state, which can only occur if the ionic site does not have inversion symmetry[10]. This 'stereochemical activity of the lone pair' is the driving force for off-centre distortion in the group IV chalcogenides[11] (for example GeTe) and in Bi-based perovskites, such as $BiMnO_3$ and $BiFeO_3$ (refs 12 and 13, respectively). Sometimes both mechanisms occur in the same material, for example in $PbTiO_3$ (recently visualized directly in electron-density maps obtained using X-ray powder diffraction[14]), and $Na_{0.5}Bi_{0.5}TiO_3$ (ref. 15). Until recently, all known magnetic ferroelectrics were thought to need lone-pair activity to introduce the ferroelectricity[9]. $TbMnO_3$ has been shown to have a small ferroelectric polarization that results from magnetoelectric coupling to the incommensurate sinusoidal antiferromagnetic ordering[16].

In this paper, we present evidence that the ferroelectricity in the hexagonal manganite, $YMnO_3$, arises from a fundamentally different mechanism. Using a combination of single-crystal X-ray diffraction (measured on an Enraf-Nonius CAD-4F diffractometer, using monochromated Mo Kα radiation) and density-functional computations, we confirm that the ferroelectricity in $YMnO_3$ arises from a buckling of the MnO_5 polyhedra (analogous to the $GdFeO_3$ rotation observed in many cubic perovskite oxides[17–19]), combined with the unusual Y coordination and the triangular and layered MnO_5 network. In striking contrast to the two established mechanisms described above, there is no re-hybridization or change in chemical bonding between the para- and ferroelectric phases. In addition to being of fundamental interest, this mechanism offers a new route for designing magnetic ferroelectrics that have been historically difficult to achieve, but are appealing for 'spintronics' applications.

The hexagonal structure adopted by $YMnO_3$ and the manganites of the small rare earths consists of non-connected layers of MnO_5 trigonal bipyramids corner-linked by in-plane oxygen ions (O_P), with apical oxygen ions (O_T) forming close-packed planes separated by a layer of Y^{3+} ions. Schematic views of the crystal structure are given in Fig. 1 and Fig. 2. We emphasize that although this structure has sometimes been described as a hexagonal perovskite structure in the literature, this is in fact a poor choice of phrase, as it is markedly different from the cubic perovskite structure, which features MnO_6 octahedra corner-linked to form a three-dimensional (3D) network. Indeed we will show that the 2D layered structure is essential for the formation of the ferroelectric state.

Early work in the 1960s established $YMnO_3$ to be ferroelectric[20,21], with space group $P6_3cm$, and revealed an A-type antiferromagnetic ordering with non-collinear Mn spins oriented in a triangular arrangement[22,23]. The coexistence of magnetism and ferroelectricity is rare, particularly in materials lacking lone pairs, and recent reports[5,24] of coupling between the magnetic and ferroelectric ordering in $YMnO_3$ provide compelling motivation for understanding the origin of its ferroelectric behaviour. In the 1970s, the high-temperature crystal structure of $YMnO_3$ was investigated[25], and a change in symmetry above the ferroelectric ordering temperature was observed. However Raman and infra-red spectroscopy of the high-temperature paraelectric and low-temperature ferroelectric phases showed only weak bands in the ferroelectric phase due to the non-centrosymmetricity, indicating that the structural differences between the ferroelectric and paraelectric phases are very small[26].

Although the studies described above correctly identified $YMnO_3$ to be ferroelectric, a thorough understanding of the crystal structure, including the crystallographic origin of the ferroelectric properties, has not yet been presented. Indeed, the early structure determinations incorrectly concluded that the ferroelectric polarization arises from an off-centre distortion of the Mn ion towards one of the apical oxygen ions. (The two Mn–O_T distances in closely related $LuMnO_3$ have been reported[20] to be 1.84 Å and 1.93 Å, in violation of the 'd^0-ness' criterion for transition metal off-centring[9]). However, the early diffraction experiments did not include the anomalous scattering contributions, which are essential for twinned, non-centred crystals. Instead, our single-crystal X-ray diffraction experiments, using reflections of the entire Ewald sphere, on several hexagonal manganites[27,28], correctly analyse such contributions, and show that the Mn ions remain very close to the centre of the oxygen bipyramids.

We find that the main difference between the paraelectric $P6_3/mmc$ and ferroelectric $P6_3cm$ structures is that in the paraelectric phase, all ions are constrained to planes, parallel to the *ab* plane, whereas below the ferroelectric transition temperature, the mirror planes perpendicular to the hexagonal *c* axis are lost. There are two major atomic displacements in the crystal structure from the centrosymmetric $P6_3/mmc$ to the ferroelectric $P6_3cm$. The first change is the buckling of the MnO_5 bipyramids, which results in a shorter *c* axis. Furthermore, due to the buckling, O_T ions are shifted in-plane towards the two longer Y–O_P bonds. The second change is the vertical shift of the Y ions away from the high-temperature mirror plane, while keeping the distance to O_T constant. Both the bond lengths within the MnO_5 bipyramids and the Y–O_T bond lengths within the sixfold coordination remain unchanged. As a result, one of the two ~2.8 Å Y–O_P bond lengths is reduced to ~2.3 Å, the other is enlarged to 3.4 Å, leading to a net electric polarization. Recent neutron-powder-diffraction experiments[29,30] also recognize the asymmetric environment of the Y ions, however they report Mn–O bond lengths that suggest off-centring of the Mn ion.

To confirm our experimental results, particularly in light of their conflict with earlier reports, we calculated the minimum energy structure using first-principles density-functional theory[31,32]. We used our self-interaction-corrected[32] ultrasoft pseudopotential implementation, as standard local-spin-density methods fail to obtain a bandgap for $YMnO_3$ (ref. 34). First, we evaluated the lattice parameters by total energy minimization of the structure within the paraelectric ($P6_3/mmc$) symmetry, assuming A-type antiferromagnetic magnetic ordering. Subsequently, we lifted the inversion symmetry to determine the atomic coordinates of the ferroelectric structure by force minimization. Our calculated atomic positions (Fig. 3) are in excellent agreement with our experimental results[27,28], and our calculated ferroelectric polarization (6.2 μC cm^{-2}) is close to the measured value[3] (5.5 μC cm^{-2}). In particular, we find that off-centring of the Mn ion, as reported previously[20], is energetically unfavourable.

As neither Y^{3+} nor Mn^{3+} has a lone pair of electrons, we know that lone-pair stereochemical activity cannot be the driving force for ferroelectricity in $YMnO_3$. Therefore the only possible chemical

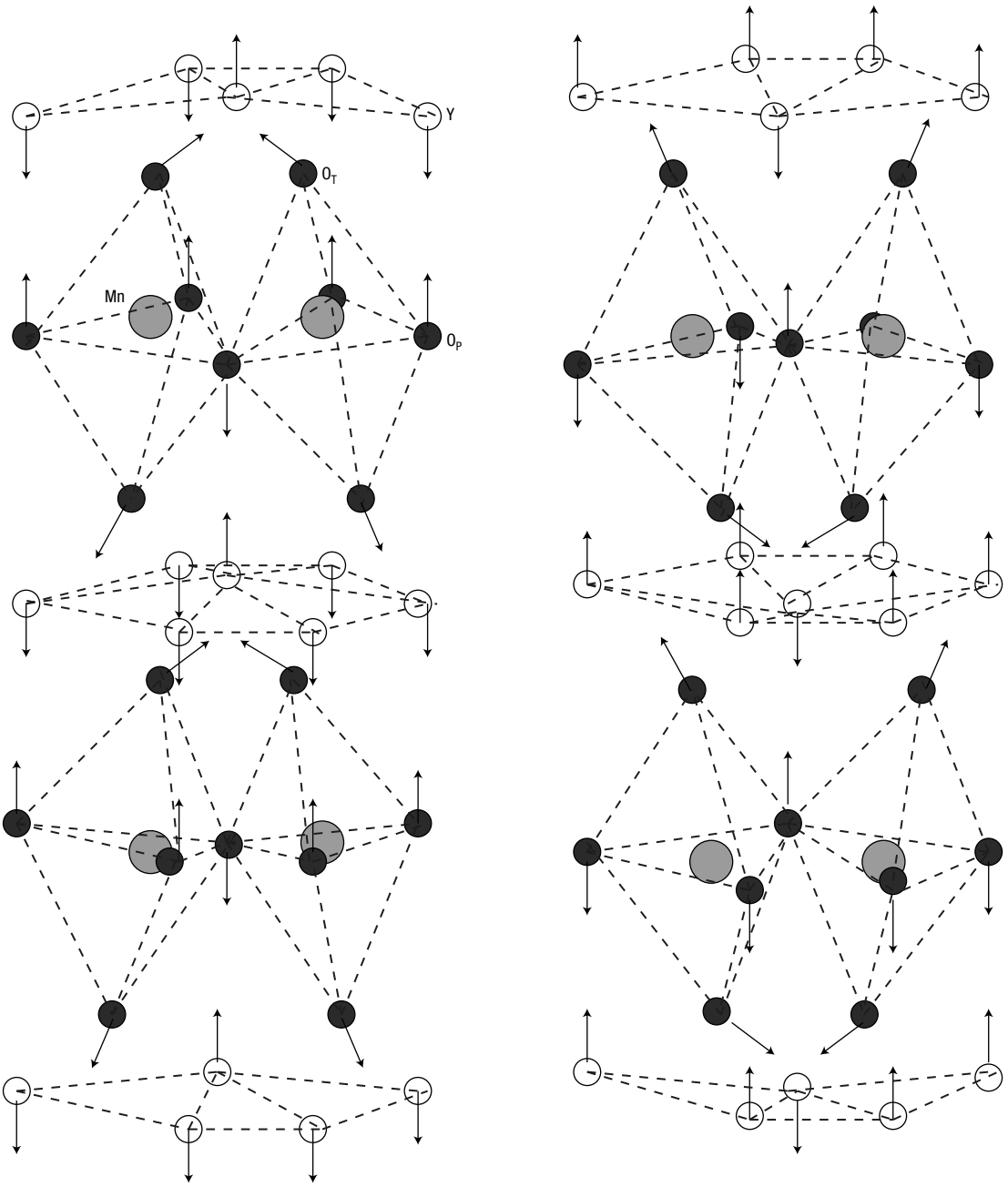

Figure 2 Three-dimensional schematic view of $YMnO_3$ in the two enantiomorphous polarized states. Arrows indicate the directions of the atomic displacements moving from the centrosymmetric to the ferroelectric structure.

mechanism is ligand-field hybridization. However, as the Mn ions remain close to the centre of their oxygen cages (in the computations they move by ~0.01 Å along the *c* axis, and remain almost unchanged in-plane), it is highly unlikely that they re-hybridize with the surrounding oxygen anions during the phase transition. And the strong off-centre displacement that occurs between Y and in-plane O_P ions, leaves the Y and O ions ~2.3 Å apart, the distance expected for a fully ionic bond[35] (compare Y_2O_3 where the average Y–O bond length is 2.27 Å). In this final part of the paper we explore the details of the ferroelectric phase transition.

To investigate chemical activity, two fundamental quantities can be calculated efficiently from first-principles: the (transverse) Born effective charges (Z^*) and the orbital-resolved densities of states. The Z^* can be defined as the atomic position derivative of the polarization at zero macroscopic electric field, or the linear-order coefficient between the electric field and the force that the field exerts on an ion at zero displacement. A large Z^* indicates that the force acting on a given ion due to the electric field generated by the atomic displacements is large even if the field is small, thus favouring the tendency towards a polarized ground state. Previous work on ferroelectric perovskite oxides[36–40] has

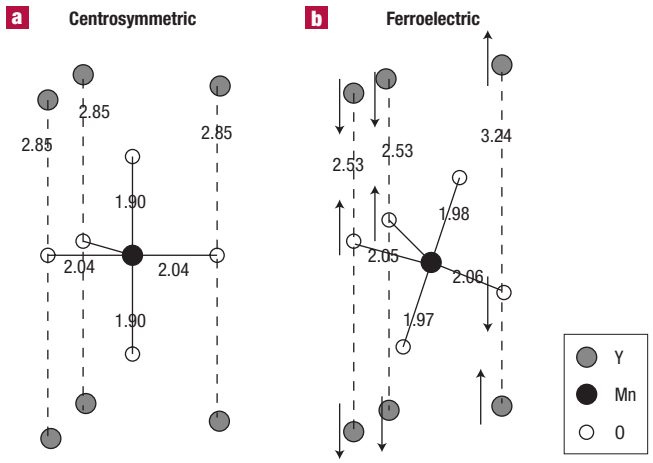

Figure 3 Schematic of a MnO_5 polyhedron with Y layers above and below. **a**,**b**, The calculated atomic positions of the centrosymmetric (**a**) and ferroelectric structures (**b**). The numbers give the bond lengths in Å. The arrows indicate atomic displacements with respect to the centrosymmetric structure.

clearly shown that in all such ferroelectrics studied, the Z^*s on the ions that displace during the phase transition are 'anomalous', in that they are far larger than (often almost double) the nominal ionic charges.

We calculated the Z^*s for $YMnO_3$ using the Berry phase approach[41–43] generalized to the case of spin-polarized systems. Our calculated values are $Z^*_Y = +3.6$, $Z^*_{Mn} = +3.3$, $Z^*_{O_T} = -2.3$, $Z^*_{O_P} = -2.2$. Thus, the Z^*s for both the O and the Mn are very close to the formal ionic charges O^{2-} and Mn^{3+}, whereas Z^*_Y is only moderately larger than the nominal Y^{3+}. The close-to-formal Z^* values for Mn and O_T ions are consistent with the absence of substantial Mn off-centre displacement with respect to the surrounding oxygen ions. Furthermore, the close-to-formal values for Y and O_P suggest that their relative displacements (which in large part cause the structure to be ferroelectric) are not driven by chemical activity such as charge transfer, rehybridization of covalent bonds, or intra-atomic redistribution of charge density. This is, to our knowledge, the first calculation of close-to-formal Z^*s on the active ions in a known ferroelectric material, and explains in part why the polarization of $YMnO_3$ is smaller than that in typical cubic perovskite ferroelectrics (in $BaTiO_3$ it is 25 μC cm^{-2} and in $PbTiO_3$, 75 μC cm^{-2}.) To explain the normal Z^*s, we show in Fig. 4 the calculated orbital-resolved density of states (DOS) for the paraelectric structure. The overlapping DOSs indicate bonding between the Mn 3*d* and O 2*p* states, but there is clearly very little interaction between the Y and O orbitals. The DOS calculated in the ferroelectric phase (not shown) is very similar to that of the paraelectric phase, confirming that there is no significant rehybridization. In particular, there is still no bonding between Y and O, which remain spatially distant even in the ferroelectric phase. In Table 1, the calculated static charges (that is, the integrals of the respective DOS components) for some representative orbitals are reported for both paraelectric and ferroelectric structures. These numbers confirm that no charge transfer occurs during the phase transition.

We now identify the actual mechanism for the large Y–O_P displacements that occur in the ferroelectric state. The total deformation can be decomposed into two components, summarized in Table 2. (Note that these are the Fourier-transforms of our calculated ferroelectric displacement vector, rather than normal modes.) One, with group theoretical symmetry label K_3, is the tilting of the Mn–O_T polyhedra, which causes a tripling of the paraelectric unit cell, and by symmetry does not lead to an overall polarization. (Although it creates large local dipole moments, these sum to zero, that is, $2dY_2 + dY_1 = 0$, and $2dO_{P2} + dO_{P1} = 0$, where d is the displacement along the c axis). The other is the so-called Γ-point component (with symmetry label Γ_1), in which the atomic displacement patterns in each unit cell are identical, and therefore can sum to give a net ferroelectric polarization. The Γ component involves primarily the Y–O_P displacements and the non-cancelling contribution of the MnO_5 rotational bucklings. Although the 'local' dipole moments are large, the moments on Y_1 are partially cancelled by their antiparallel ordering to the moments on Y_2. This also contributes to the relatively low polarization. Group theoretical analysis and high-temperature diffraction[44,45] shows that the transition from the paralectric $P6_3/mmc$ to the ferroelectric $P6_3cm$ phase in fact takes place in two steps. (This is consistent with earlier reports[25,30] of no structural phase transition at the ferroelectric Curie temperature, T_c.) As temperature is reduced, the unit cell-tripling K_3 mode first lowers the symmetry, but does not lead to a ferroelectric polarization. At a significantly lower temperature, the ferroelectric transition takes place without further reduction in symmetry.

In Fig. 5, we report the calculated energies as a function of the structural distortion for both the total ferroelectric displacement and its Γ-point component. (The difference between the two curves is the contribution from the buckling of the oxygen cages). Both curves present the well-known double-well shape around the centrosymmetric point, indicating that both the Γ-point uniaxial Y–O_P ferroelectric displacements and the K_3 tiltings are independently energetically

Table 1 Static charges of selected orbitals calculated for the paraelectric and ferroelectric structure of $YMnO_3$.

	Y p_z	Y d_{z2}	O_P p_z	O_T p_z	Mn d_{z2}
Paraelectric	0.08	0.09	0.90	0.85	0.51
Ferroelectric	0.08	0.11	0.90	0.85	0.53

Table 2 Calculated ferroelectric displacements along the *c* axis (TOT_{calc}), and the Fourier-space projections calculated at the zone-centre (Γ_1) and the zone-boundary (K_3) of the paraelectric Brillouin zone.

Atom	Γ_1	K_3	TOT_{calc}
Y_1	–0.0439	0.1480	0.1222
Y_2	–0.0439	–0.0740	–0.0995
O_T	0.1551	0	0.0894
Mn	0.0206	0	0.0116
O_{P1}	0.0984	–0.3233	–0.2667
O_{P2}	0.0984	0.1617	0.2186
O_T	–0.0799	0	–0.0460

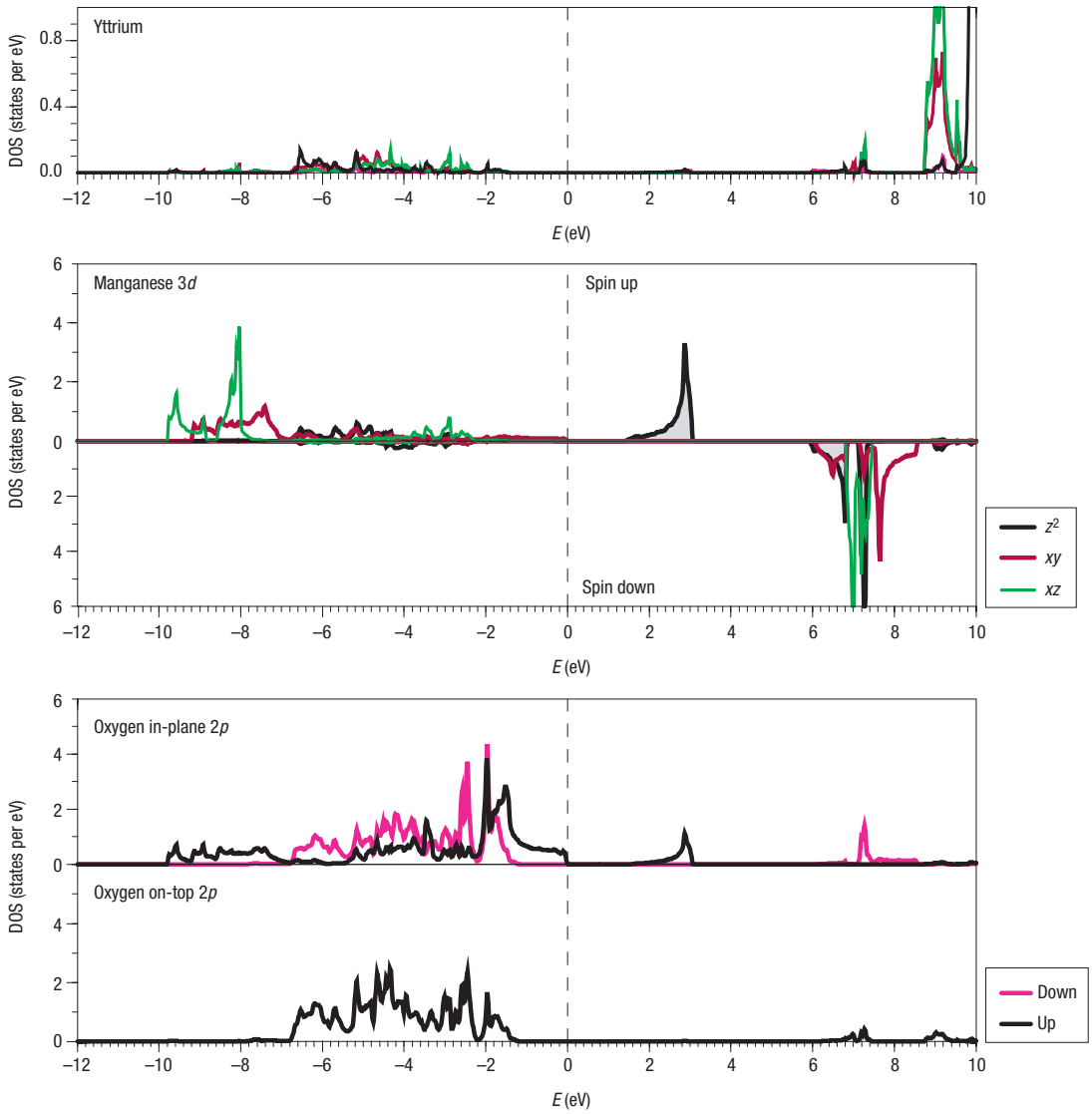

Figure 4 Orbital-resolved densities of states of Mn, O and Y ions for paraelectric $YMnO_3$. The overlapping DOSs indicate bonding between the Mn 3*d* and O 2*p* states, but there is clearly very little interaction between the Y and O orbitals. The DOS calculated in the ferroelectric phase (not shown) is very similar to that of the paraelectric phase, confirming that there is no significant rehybridization.

favoured with respect to the centrosymmetric structure. The tilting of the $Mn–O_T$ bonds, although not generating a polarization directly, cooperates with the $Y–O_P$ displacements to contribute a large part of the energy lowering between paraelectric and ferroelectric states. It also enlarges the displacement at which the energy is at a minimum. The total energy lowering is ~60 meV per formula unit, which corresponds to T_c ~700 K, consistent with the experimental value. Note that neither distortion is associated with chemical rehybridization, but instead both are stabilized by electrostatic and size effects.

It is important to emphasize that the role of the Mn–O polyhedral rotations in stabilizing the ferroelectric structure is in striking contrast to the situation in the ABO_3 cubic perovskites. Such rotations are widely observed in cubic perovskites. For example in $LaMnO_3$, $GdFeO_3$ and YVO_3, there is a rotation of the BO_6 octahedra, and a shift of the A cations from their pseudocubic sites[17,18,46]. The A cations become acentrically coordinated with respect to the oxygen ions and the inversion symmetry with respect to a reference system centred on the A ion is lost. However, as a result of the 3D connectivity, a rotation of the polyhedra around a particular lattice axis forces the corner-linked polyhedra in the two perpendicular directions to rotate in the opposite direction[17]. Therefore the global inversion symmetry is retained. As a consequence, no electric polarization occurs (such materials are sometimes referred to as anti-ferroelectrics). Some materials, such as $(Na,Bi)TiO_3$, do show oxygen cage rotations and ferroelectricity; however, the ferroelectricity—which is driven by the usual off-centring of the Ti^{4+} ion and the lone-pair active Bi^{3+} ion[15]—in this case occurs in spite of the rotations. In $YMnO_3$, instead, due to the layered structure and the triangular symmetry, the rotations break the inversion symmetry and lower the symmetry to that of the ferroelectric phase.

Finally, we point out that our findings are not only relevant to $YMnO_3$. Indeed, it was predicted that a further eight ABO_3 compounds from the $YMnO_3$ family will show ferroelectricity[47], which, if correct, will probably be explained with the same arguments. And ferroelectricity has been predicted to occur in perovskite

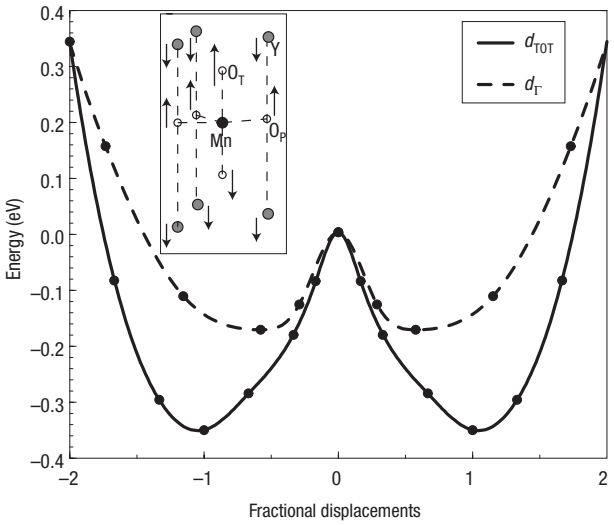

Figure 5 Energies as a function of the atomic displacements from their centrosymmetric positions. Fractional displacements of ±1 correspond to the calculated ferroelectric minima. d_{TOT} represents the total displacement and d_{Γ} its Γ point component. The inset shows the Γ point component, with the arrows indicating the magnitude of the displacements along the *c* axis from the centrosymmetric structure. Note that in spite of the relative motions along the *c* axis, the Mn ions remain in the centre of their oxygen polyhedra (that is, the Mn–O bond lengths are nearly unchanged from their values in the centrosymmetric structure) because of large oxygen displacements in the *ab* plane (K_3 mode), which are not shown here and which do not contribute to the polarization.

structure $NaCaF_3$, accompanied by polyhedral CaF_3 rotations[48] and close-to-formal Z^*s (ref. 49). Also, tris-sarcosine calcium chloride, $(CH_3NHCH_2COOH)_3CaCl_2$, is a uniaxial ferroelectric whose order parameter involves rotation of sarcosine molecules out of the paraelectric mirror plane. It is reported to have an unusually small splitting between the longitudinal and optical phonon modes[50], which is consistent with the non-anomalous Z^*s that we obtain for ferroelectrics adopting the mechanism described here. And a rotational ferroelectric soft mode has been reported in some so-called 'weak ferroelectrics' such as lithium germanate[51] ($Li_2Ge_7O_{15}$). We point out, however, that the spontaneous polarizations in these latter materials are two orders of magnitude smaller than that of $YMnO_3$.

In summary, our results for structural and electronic properties give a consistent picture of $YMnO_3$ as an anomalous ferroelectric oxide, for which rehybridization and covalency play a minor role (or no role at all) in the ferroelectric transition. Instead, long-range dipole–dipole interactions and oxygen rotations both cooperate to drive the system towards the stable ferroelectric state. Indeed, the huge Y–O_P off-centre displacements are quite distinct from the small displacements driven by chemical activity found in conventional ferroelectric perovskites, and represent a completely different mechanism for ferroelectric distortion. The polarization is a consequence of the unusual Y-site coordination and the triangular and layered MnO_5 network. Furthermore, this mechanism suggests a new route for designing magnetic ferroelectric bulk or thin-film materials, as it permits the presence of magnetic ions in the ferroelectric phase.

Received 28 November 2003; accepted 22 January 2004; published 22 February 2004.

References

1. Auciello, O., Scott, J. F. & Ramesh, R. The physics of ferroelectric memories. *Phys. Today* **51,** 22–27 (1998).
2. Busch-Vishniac, I. J. Trends in electromechanical transduction. *Phys. Today* **51,** 28–34 (1998).
3. Fujimura, N., Ishida, T., Yoshimura, T. & Ito, T. Epitaxially grown $YMnO_3$ film: New candidate for nonvolatile memory devices. *Appl. Phys. Lett.* **69,** 1011–1013 (1996).
4. Ito, D., Fujimura, N., Yoshimura, T. & Ito, T. Ferroelectric properties of $YMnO_3$ epitaxial films for ferroelectric-gate field-effect transistors. *J. Appl. Phys.* **93,** 5563–5567 (2003).
5. Fiebig, M., Lottermoser, T., Fröhlich, D., Goltsev, A. V. & Pisarev, R. V. Observation of coupled magnetic and electric domains. *Nature* **419,** 818–820 (2002).
6. Ok, K. M., Bhuvanesh, N. S. P. & Halasyamani, P. S. Bi_2TeO_5: Synthesis structure and powder second harmonic generation properties. *Inorg. Chem.* **40,** 1978–1980 (2001).
7. Cohen, R. E. & Krakauer, H. Electronic-structure studies of the differences in ferroelectric behavior of $BaTiO_3$ and $PbTiO_3$. *Ferroelectrics* **136,** 65–83 (1992).
8. Cohen, R. E. Origin of ferroelectricity in perovskite oxides. *Nature* **358,** 136–138 (1992).
9. Hill, N. A. Why are there so few magnetic ferroelectrics? *J. Phys. Chem. B* **104,** 6694–6709 (2000).
10. Atanasov, M. & Reinen, D. Density functional studies on the lone pair effect of the trivalent group V elements: I. electronic structure, vibronic coupling, and chemical criteria for the occurrence of lone pair distortions in AX_3 molecules (A=N to Bi; X=H, and F to I). *J. Phys. Chem. A* **105,** 5450–5467 (2001).
11. Waghmare, U. V., Spaldin, N. A., Kandpal, H. C. & Seshadri, R. First principles indicators of metallicity and cation off-centricity in the IV-VI rock-salt chalcogenides of divalent Ge, Sn and Pb. *Phys. Rev. B* **67,** 125111 (2003).
12. Seshadri, R. & Hill, N. A. Visualizing the role of Bi 6s "lone pairs" in the off-center distortion in ferromagnetic $BiMnO_3$. *Chem. Mater.* **13,** 2892–2899 (2001).
13. Wang, J. *et al.* Epitaxial $BiFeO_3$ multiferroic thin film heterostructures. *Science* **299,** 1719–1722 (2003).
14. Kuroiwa, Y. *et al.* Evidence for Pb-O covalency in tetragonal $PbTiO_3$. *Phys. Rev. Lett.* **87,** 217601 (2001).
15. Jones, G. O. & Thomas, P. A. Investigation of the structure and phase transitions in the novel a-site substituted distorted perovskite compound $Na_{0.5}Bi_{0.5}TiO_3$. *Acta Crystallogr. B* **58,** 168–178 (2002).
16. Kimura, T. *et al.* Magnetic control of ferroelectric polarization. *Nature* **426,** 55–58 (2003).
17. Glazer, A. M. The classification of tilted octahedra in perovskites. *Acta Crystallogr. B* **28,** 3384–3392 (1972).
18. Van Aken, B. B., Meetsma, A., Tomioka, Y., Tokura, Y. & Palstra, T. T. M. Structural response to O*-O' and magnetic transitions in orthorhombic perovskites. *Phys. Rev. B* **66,** 224414 (2002).
19. Van Aken, B. B. *Structural Response to Electronic Transitions in Hexagonal and Ortho-manganites* Thesis, Univ. Groningen (2001).
20. Yakel, H. L., Koehler, W. C., Bertaut, E. F. & Forrat, E. F. On the crystal structure of the manganese (III) trioxides of the heavy lanthanide and yttrium. *Acta Crystallogr.* **16,** 957–962 (1963).
21. Smolenskii, G. A. & Bokov, V. A. Coexistence of magnetic and electric ordering in crystals. *J. Appl. Phys.* **35,** 915–918 (1964).
22. Bertaut, E. F., Pauthenet, R. & Mercier, M. Proprietes magnetiques et structures du manganite d'yttrium. *Phys. Lett.* **7,** 110–111 (1963).
23. Bertaut, E. F., Pauthenet, R. & Mercier, M. Sur des proprietes magnetiques du manganite d'yttrium. *Phys. Lett.* **18,** 13 (1965).
24. Lottermoser, T., Fiebig, M., Fröhlich, D., Kallenbach, S. & Maat, M. Coupling of ferroelectric and antiferromagnetic order parameters in hexagonal $RMnO_3$. *Appl. Phys. B* **74,** 759–764 (2002).
25. Łukaszewicz, K. & Karut-Kalicinska, J. X-ray investigations of the crystal structure and phase transitions of $YMnO_3$. *Ferroelectrics* **7,** 81–82 (1974).
26. Iliev, M. N. *et al.* Raman- and infrared-active phonons in hexagonal $YMnO_3$: Experiment and lattice-dynamical calculations. *Phys. Rev. B* **56,** 2488–2494 (1997).
27. Van Aken, B. B., Meetsma, A. & Palstra, T. T. M. Hexagonal $YMnO_3$. *Acta Crystallogr. C* **57,** 230–232 (2001).
28. Van Aken, B. B., Meetsma, A. & Palstra, T. T. M. Hexagonal $LuMnO_3$ revisited. *Acta Cryst. E* **57,** i38–i40 (2001); ibid. i87–i89; ibid. i101–i103.
29. Muñoz, A. *et al.* Magnetic structure of hexagonal $RMnO_3$ (R = Y, Sc): thermal evolution from neutron powder diffraction. *Phys. Rev. B* **62,** 9498–9510 (2000).
30. Katsufuji, T. *et al.* Crystal structure and magnetic properties of hexagonal $RMnO_3$ (R = Y, Lu and Sc) and the effect of doping. *Phys. Rev. B* **66,** 134434 (2002).
31. Hohenberg, P. & Kohn, W. Inhomogeneous electron gas. *Phys. Rev.* **136,** 864–871 (1964).
32. Kohn, W. & Sham, L. J. Self-consistent equations including exchange and correlation effects. *Phys. Rev.* **140,** 1133–1138 (1965).
33. Filippetti, A. & Spaldin, N. A. Self-interaction corrected pseudopotential scheme for magnetic and strongly-correlated systems. *Phys. Rev. B* **67,** 125109 (2003).
34. Filippetti, A. & Hill, N. A. Coexistence of magnetism and ferroelectricity in perovskites. *Phys. Rev. B* **65,** 195120 (2002).
35. Shannon, R. D. & Prewitt, C. T. Revised effective ionic radii and systematic studies of interatomic distances in halides and chalcogenides. *Acta Crystallogr. A* **32,** 751–767 (1976).
36. Zhong, W., King-Smith, R. D. & Vanderbilt, D. Giant LO-TO splittings in perovskite ferroelectrics. *Phys. Rev. Lett.* **72,** 3618–3621 (1994).
37. Ghosez, P., Michenaud, J.-P. & Gonze, X. Dynamical atomic charges: The case of ABO_3 compounds. *Phys. Rev. B* **58,** 6224–6240 (1998).
38. Resta, R., Posternak, M. & Baldereschi, A. Towards a quantum-theory of polarization in ferroelectrics - the case of $KNbO_3$. *Phys. Rev. Lett.* **70,** 1010–1013 (1993).
39. Posternak, M., Resta, R. & Baldereschi, A. Role of covalent bonding in the polarization of perovskite oxides - the case of $KNbO_3$. *Phys. Rev. B* **50,** 8911–8914 (1994).
40. Ghosez, P., Gonze, X. & Michenaud, J.-P. First principles calculations of dielectric and effective charge tensors in barium titanate. *Ferroelectrics* **153,** 91–96 (1994).
41. King-Smith, R. D. & Vanderbilt, D. Theory of polarization of crystalline solids. *Phys. Rev. B* **47,** R1651–R1654 (1993).

42. Resta, R. Macroscopic electric polarization as a geometric quantum phase. *Eur. Phys. Lett.* **22,** 133–138 (1993).
43. Resta, R. Macroscopic polarization in crystalline dielectrics: the geometric phase approach. *Rev. Mod. Phys.* **66,** 899–915 (1994).
44. Lonkai, T. *Electric and Magnetic Order Parameter in the Multiferroic Hexagonal $RMnO_3$ System* Thesis, Tübingen Univ. (2003).
45. Tomuta, D. *Investigations of Hexagonal Manganites with Magnetic and Non-Magnetic Rare Earths* Thesis, Univ. Leiden (2003).
46. Mizokawa, T., Khomskii, D. I. & Sawatzky, G. A. Interplay between orbital ordering and lattice distortions in $LaMnO_3$, YVO_3, and $YTiO_3$. *Phys. Rev. B* **60,** 7309–7313 (1999).
47. Abrahams, S. C. Ferroelectricity and structure in the $YMnO_3$ family. *Acta Crystallogr. B* **57,** 485–490 (2001).
48. Edwardson, P. J. *et al.* Ferroelectricity in perovskitelike $NaCaF_3$ predicted ab initio. *Phys. Rev. B* **39,** 9738–9741 (1989).
49. Boyer, L. L. *et al.* Predicted properties of $NaCaF_3$. *AIP Conf. Proc.* **535,** 364–371 (2000).
50. Kozlov, G. V., Volkov, A. A., Scott, J. F., Feldkamp, G. & Petzelt, J. Millimeter-wavelength spectroscopy of the ferroelectric phase transition in tris-sarcosine calcium chloride $(CH_3NHCH_2COOH)_3CaCl_2$. *Phys. Rev. B* **28,** 255–261 (1983).
51. Iwata, Y., Shibuya, I., Wada, M., Sawada, A. & Ishibashi, Y. Neutron diffraction study of structural phase transition in ferroelectric $Li_2Ge_7O_{15}$. *J. Phys. Soc. Jpn* **56,** 2420–2427 (1987).

Acknowledgements

We thank Neil Mathur, Jim Scott, Ron Smith and Auke Meetsma for invaluable discussions and experimental assistance. The work by A.F. and N.A.S. on this project was funded by the US National Science Foundation's Division of Materials Research, grant number DMR-0312407. This work is supported by the Stichting voor Fundamenteel Onderzoek der Materie (FOM). Beam time at ISIS Rutherford Appleton Laboratory, Chilton, Didcot, UK was funded by Nederlandse Organisatie voor Wetenschappelijk Onderzoek (NWO). A.F. acknowledges funding from the Italian Ministry of Research (MIUR) under the Rentro Cervelli 2002 program.
Correspondence and requests for materials should be addressed to N.A.S.

Competing financial interests

The authors declare that they have no competing financial interests.